THE ASTROPHYSICAL JOURNAL, 392:74–79, 1992 June 10

FROM FAIRALL 9 TO HIGH-z OBJECTS: PATTERN OF CHANGE IN IONIZATION STRUCTURE

WEI ZHENG
Department of Physics and Astronomy, University of Alabama, Tuscaloosa, AL 35487-0324, and Center for Astrophysical Sciences, Johns Hopkins University, Baltimore, MD 21218
LI-ZHI FANG
Department of Physics and Steward Observatory, University of Arizona, Tucson, AZ 85721
AND
LUC BINETTE
Canadian Institute for Theoretical Astrophysics, 60 St. George Street, Toronto, Canada, ON M5S 1A1
Received 1991 January 7; accepted 1991 December 17

ABSTRACT

A study of 79 *IUE* spectra of the Seyfert galaxy Fairall 9 shows a considerable change in the continuum shape which can be characterized by several sections. The flux at 3075 Å changes in approximate proportion to the optical and X-ray flux, suggesting that they may be a part of the power law. The apparent fourfold change in the continuum slope between 1826 and 3075 Å indicates a considerably different variations for the UV bump and the power-law continuum. The most variable part between 1338 and 1826 Å keeps a constant slope.

Significant differential variations are found in weaker emission lines, including N v λ1240, Si iv λ1400, He ii λ1640, and C iii] λ1909. Low-ionization lines (threshold energy between 1 and 3 Ry) appear to follow the UV bump, and high-ionization lines follow the power-law continuum. The results, in addition to the previous report on strong lines, suggest that the variation amplitude of lines is inversely correlated to the effective excitation level. Our multiline fit suggests that the UV bump has a shape more complicated than a simple blackbody curve and its high-energy tail extends beyond 3 eV.

An active galactic nucleus statistic finds that the degree of luminosity dependence of equivalent width is inversely correlated with individual emission line's excitation level. This offers a natural explanation as to why the C iv equivalent width shows the most significant luminosity dependence (the Baldwin effect). We suggest a more prominent UV bump in high states or in high-luminosity objects.

Subject headings: galaxies: individual (Fairall 9) — galaxies: nuclei — galaxies: Seyfert — ultraviolet: galaxies

1. INTRODUCTION

Photoionization models in which UV and X-ray photons are the dominant energy input to the excited plasma are reasonably successful in explaining the observed relation between emission line and continuum intensities. However, until recently, most studies on the variability of the emission lines in active galactic nuclei (AGNs) have *assumed* that the extreme ultraviolet (EUV) and the X-ray components vary in phase and with equal amplitude with the optical and UV counterparts. Such a simplified assumption is clearly at odds with current multiband variability observations of well-studied AGNs. For example, Clavel, Wamsteker, & Glass (1989) show that the UV continuum level in the Seyfert 1 galaxy Fairall 9 (F9, $z = 0.045$) has varied by a factor of 33, while the soft X-ray variations appear not to have exceeded a factor 3–4 during the same period. Changes in energy distribution have also become apparent in the Seyfert 1 galaxy NGC 5548 where coordinated multiband observations (Clavel et al. 1991; Peterson et al. 1991) have shown that the UV continuum is harder at high states.

Furthermore, the response of the Lyα/C iv ratio to the continuum variability is in clear contradiction to the expectations of the standard photoionization model. A successful model of the Lyα/C iv response is obtained by Binette et al. (1989) and Clavel & Santos-Lleó (1990) only after decoupling the soft X-ray variation from that of the EUV. The suggestion of relating the emission line response to the existence of semi-independent UV and soft X-ray components may have fundamental implications for the study of different mechanisms producing the observed energy distribution.

The response of Lyα/C iv, and other lines to continuum variability provides us with a powerful test of photoionization models and should lead us to a better understanding of the physical conditions characterizing the broad-line region. It is interesting to note that correlations between line and continuum variations have also been inferred from statistical studies of AGN data. For instance, a relation between continuum luminosity and Lyα/C iv ratio has been found in the low-luminosity Seyfert galaxies (Kinney et al. 1987) as well as in the high-luminosity QSOs (Baldwin, Wampler, & Gaskell 1989). Such a luminosity-dependence appears to coexist with the anti-correlation between C iv equivalent width (EW) and continuum luminosity (the Baldwin effect, Baldwin 1977).

2. RESULTS

2.1. *Data*

More than 100 *IUE* archival spectra of F9 obtained between 1978 and 1987 have been retrieved. The majority of the data are from the NASA National Space Science Data Center (NSSDC) in the extracted MELO format. About 10 spectra are from the Rutherford-Appleton Laboratory in the UK. The sensitivity loss of the LWR camera is corrected using the algo-

TABLE 1

IUE DATA SOURCE FOR FAIRALL 9

Group	SWP		LWP/R	
1.....	1804	2178	R1685	R1954
	2215	3936	R3511	
	3937			
2.....	4732	9353	R3959	R3960
	9354	9616	R8114	R8382
3.....	10941	15794		
	15795	13616	R9615	R10000
	14157	14158	R10002	R10761
	15689	16410	R12166	R12662
	16559	16890	R13714	R13801
	17446			
4.....	17249	18506	R13514	R14585
	18382	28632	R14908	P8562
	30152	30933	P10017	P10713
	31175		P11027	
5.....	28212	28891	P7022	P7023
	29990	29992	P8080	P9425
			P9426	P9823
6.....	27399	27400	P7396	P7397
	26479	26480	P6491	P6492
	25825		P5872	
7.....	23824	24193	P4106	P4603
	24254	14291	P4639	
	24345			

rithm of Clavel, Gilmozzi, & Prieto (1988). Since Clavel et al. (1989) have made a comprehensive study of the Lyα, C IV, and Mg II lines, we have concentrated on the weaker lines and, to this effect, have produced a merged data set in order to improve the S/N level. Not every spectrum turns out to be useful, especially in the case of the long-wavelength spectra. The C III] emission falls into an unfavorable, noisy part of the LW cameras, and some *IUE* spectra of long exposure suffer saturated emission features. Each *IUE* spectrum has been inspected for its S/N level, unusual features, saturation effects, larger than normal wavelength shifts, etc. In some cases, the background counts and line-by-line images are also studied. Only those believed to be reliable have been retained: in total 41 short-wavelength and 38 long-wavelength spectra. The spectra are divided into seven groups according to preset continuum levels. The groups are assembled to assure that each merged spectrum would have a similar continuum shape and emission features. Most SWP and LW spectra correspond to data pairs which were taken only a few days apart. The continuum variation at 1388 Å within each group covers a flux range of between 1.5 to 2. The spectra within a given group are merged together using different weights, depending on the exposure time and the relative quality of the spectra. Table 1 lists the data source along with the group (i.e., continuum level) they are assigned to. All the measurements are in the observer's reference frame.

The N V measurements are made after line deconvolutions. We use a dual-Gaussian fit for the Lyα profile and a C IV template for the N V. The fittings result in a typical narrow Lyα component of FWHM $\sim$2500 km s^{-1} and a broad one of FWHM $\sim$8000 km s^{-1}. To increase reliability, a second reference continuum level around 1950 Å is measured from the corresponding SWP scan in each merged long-wavelength spectrum. The C III] line flux is measured between 1960 and 2020 Å in the LW spectra using the 1950 Å reference level. Flux measurements are presented in Table 2 in the order of decreasing energy of the ionizing photons (except for Mg II and Fe II, but see below). In the averaged spectra the emission blend between 1675 and 1775 Å is a flat feature. Although we are not able to deblend the He II emission from the O III 1663, we choose the flux measured between 1675 and 1725 Å as this part seems to always account for half of the whole emission feature. The Fe II feature refers to the bump between 2350 and 2750 Å as the underlying continuum is determined by the interpolation of flux at 2150 and 3075 Å.

Even after merging the spectra to improve the S/N, the accuracy in the line fluxes is not always satisfactory. Figure 2*a* shows the relation between renormalized line intensities and continuum. The renormalization procedure consists in dividing each series of line and continuum fluxes by their respective peak flux. The peak value usually corresponds to the data with the highest S/N level. Because of the greatly improved S/N level of the merged spectra, the flux accuracy for the Lyα, Si IV, C IV, and Mg II lines is estimated at 10% or better. The accuracy for the He II, N V, and C III] lines is estimated at 30% or better. The uncertainty of C III] intensity in level 6 and 7 is higher. During the procedure of integrating line fluxes, the underlying continuum level is estimated at four wavelength

TABLE 2

CONTINUUM AND LINE FLUX[a,b]

					IONIZATION POTENTIAL (eV)							
					8	8	77	24	48	33	24	
					EFFECTIVE EXCITATION ENERGY (eV)							
					600	500	77	54	48	33	24	13
LEVEL	*F*(1338)	*F*(1826)	*F*(2150)	*F*(3075)	Mg II	Fe II	N V	He II	C IV	Si IV	C III]	Lyα
1	214	162	96	49	28	36	19	5.0	70	26	19	262
2	148	104	74	50	31	28	18	3.5	66	29	17	243
3	91	65	42	32	26	22	16	2.8	59	18	15	162
4	72	50	33	24	20	18	12	2.6	49	14	10	137
5	47	33	23	19	15	14	9.8	1.9	37	8.6	7	78
6	30	21	17	16	14	12	8.2	1.7	31	6.7	2.9:	70
7	8.8	7.1	8	8	10	9	3.5	1.0	14	2.8	< 2	29
Max/Min	24 ± 2	23 ± 2	12 ± 2.5	6.1 ± 0.6	2.8 ± 0.4	4.0 ± 0.7	5.4 ± 1	5.0 ± 1.0	5.0 ± 0.4	9.3 ± 1.5	> 9	9.0 ± 0.8

[a] Continuum flux in units of 10^{-15} ergs cm^{-2} s^{-1} Å^{-1}, measured at given wavelength bands (Å).

[b] Line flux in units of 10^{-13} ergs cm^{-2} s^{-1}.

bands around 1338, 1826, 2150, and 3075 Å. These bands are probably the most favorable regions for minimizing line contamination and instrumental defects. The continuum measurement errors are estimated at 10%, except at 2150 Å for the middle and low states where it is estimated at 20%.

2.2. *Change in the Continuum Energy Distribution*

From 1978 to 1984, the UV continuum has undergone a general decline, which we find is accompanied by a pronounced change in slope. For instance, the flux ratio, in units of ergs cm^{-2} s^{-1} $Å^{-1}$ and measured at 1338 and 3075 Å, is 4.9 at level 1 (high state) and 1.1 at level 7, respectively.

Our results suggest that some sections of the UV energy distribution are characterized by distinct variability properties. Clavel et al. (1989) find that the spectral index between 1338 and 1826 Å remains unchanged throughout the whole range in continuum variation. Our analyses lead to the same result although we find significant changes in the spectral index longward of 1900 Å. For instance, the ratio of fluxes between 1826 and 2150 Å has varied by as much as a factor of 2.8. We might consider that the UV bump which dominates at short wavelengths is characterized by a constant spectral index while at longer wavelengths the spectral index of the continuum is affected by a distinct and less variable component. This interpretation requires the variable UV bump to be characterized by a sharp turn-on energy in order for the other underlying component to affect the optical UV continuum substantially. If this is the case, we would expect that the continuum around 3075 Å is even less affected by the UV bump and hence best represents this underlying continuum component. The abrupt deviation from a power law is not consistent with blackbody curves.

Comparing the flux at 3075 Å with the corresponding optical spectrophotometric data (Wamsteker et al. 1985), we find that between 1981 August and 1984 August, the optical continuum at 5076 Å has varied by a factor of 3.2 while our flux measurments at 3075 Å yield a very similar factor of 4 in variation (over the same epochs which correspond to levels 7 and 3). This strongly suggests that the continuum between 5000 and 3000 Å has varied very little in contrast to the dramatic changes observed at the shorter wavelengths. Considering that Morini et al. (1986) have reported a similar amplitude variation of a factor $\simeq 3$–4 for the soft X-rays, we might conjecture that the underlying continuum component at 3075 Å is simply an extension of the soft X-ray power law to which is superposed the highly variable UV bump which clearly dominates shortward of 2000 Å.

2.3. *Differential Line Variation*

Figure 1 plots the composite spectra at the highest (level 1) and lowest state (level 7). The spectra are smoothed with a filter of 3 Å. The upper plot represents typical S/N ratios for lines between level 1 and 5. In addition to the previously studied large variations in Lyα and C IV, we see that the Si IV and C III] lines are also characterized by large variations. From one continuum level to another, as we clearly see in Figure 2*a*, significant differential variations above the estimated noise level.

As shown in Table 2, the amplitude of the variations correlates approximately with the threshold energy of the ionizing photons responsible for creating the emitting species (in the case of recombination lines, the photons involved are those responsible for producing He III and H II). This ionization

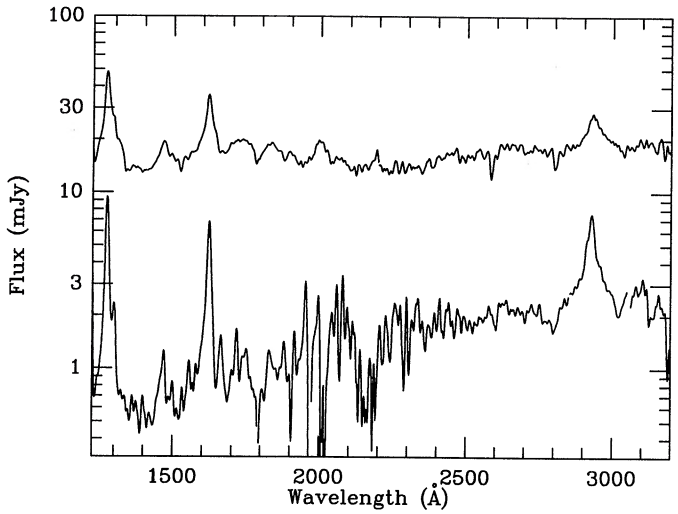

FIG. 1.—Two representative UV spectra of Fairall 9. Top and bottom curves correspond to the high state (level 1) and to the low state (level 7), respectively.

sequence, in the order of decreasing energy (but approximately increasing amplitude variation), is the following: N^{+4}, He^{+}, C^{+3}, Si^{+3}, C^{+2}, H^{+}. At first sight, it might appear that the Mg II and Fe II lines are at odds with the above trends since they are characterized by both low ionization potentials and quite small variation amplitudes. On the other hand, it is well known that the photons that create the semi-ionized zone responsible for the Mg II and Fe II emission correspond mostly to soft X-rays. Krolik & Kallman (1988) estimate the threshold energies at around 600 and 500 eV for Mg II and Fe II, respectively, which would make these lines fit nicely the above trend of inverse relation between amplitude and effective excitation energy (see Table 2). If we group together lines of similar excitation, we obtain that the high-ionization lines with ionization energy greater than 4 Ry (C IV, N V) vary approximately by a factor of 5 while the lower ionization lines with an ionization energy between 1 and 3 Ry vary by a factor of 10.

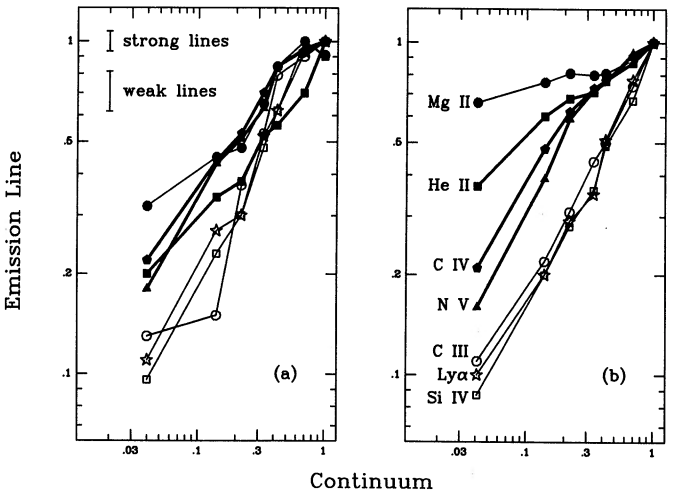

FIG. 2.—(*a*) Line fluxes as a function of continuum flux (at 1338 Å), representative error bars are for strong (Lyα, C IV, and Mg II) and weak lines respectively, and (*b*) calculated fractional changes, for Fairall 9. All line and continuum fluxes are renormalized relative to the corresponding peak value. Thicker curves represent lines for higher ionization.

Between level 1 and 5, the C III] flux is of sufficient accuracy ($\sim$20%) to allow comparison of its differential variation with that of C IV. The C III]/C IV ratio is 0.27 ± 0.05 in level 2, and 0.14 ± 0.03 in level 5. Therefore, C III] appear characterized by a larger fractional change similar to that of Lyα and Si IV. This trend is shown in Figure 2*a* in which thicker curves mark lines of higher ionization potential.

3. DISCUSSIONS

3.1. *The UV Bump Cutoff*

Based on the variation of Lyα/C IV ratio, Binette et al. (1989) and Clavel & Santos-Lleó (1990) use the spectra similar to a blackbody and find the cutoff energy around 1 Ry. Their calcualtions reproduce the critical decrease of the C IV/C III] ratio with increasing ionizing flux which can also be seen in our Figure 1*a*. Furthermore, the results of more emission lines enable us to map the bump's high-energy end.

We find that the Si IV line may be a potentially useful indicator. It resembles C IV in many aspects except for the lower ionization threshold at 33 eV. Blending with the O IV line does cause uncertainties, but with an ionization potential of 55 eV for O^{+3}, the O IV λ1402 is not expected to be significant (30% or less) at high densities ($>10^{10}$ cm^{-3}, cf. Rees, Netzer, & Ferland 1989). In F9, the high Si IV/Lyα ratio of $\sim$0.1 does imply such a high density as the Lyα emission becomes less efficient due to strong radiative transfer. Furthermore, the Si IV/Lyα ratio, like C IV and other high-ionization lines, is also sensitive to the ionization parameter in case of a power law. If the UV bump is not to extend at all beyond 33 eV, the Si IV emission would be entirely dependent on the strength of the underlying power-law continuum and therefore would vary more or less in the same proportion as C IV (that is, more than Lyα). If anything, however, the observed Si IV/Lyα ratio appears to increase toward the high state. This suggests that the high-energy tail of the bump should be able to ionize Si^{+2} but not C^{+2}.

To extend the comparison to weaker lines, we have repeated the calculations with a 10 eV UV bump using the code *MAPPINGS* (Binette, Robinson, & Courvoisier 1988) modified to a high-density regime. Details of the calculations can be found in Binette et al. (1989). The abundances are solar, the hydrogen density of the photoionized gas condensations is 3×10^{10} cm^{-3}, and the ionization parameter at low state is $U = 0.02$. The bump spectrum is represented by

$$f_\nu \propto \nu^{1/3} e^{-h\nu/E_{eV}} .$$

Noting that a significant drop does not take place immediately at $h\nu = E_{eV}$, the model of Binette et al. actually implies a significant decline of bump flux beyond 20 eV. To accommodate the observed change in the power-law continuum from optical to X-ray energies, we assume that the underlying power-law continuum varies threefold while the UV bump varies by a factor of 30. This results in a composite UV continuum which varies by a factor of 24 round 1338 Å. The calculated line variations for $E_{eV} = 8$ eV are shown in Figure 2*b*. The pattern for the variations qualitatively mimics those observed.

By varying the cutoff energy E_{eV}, we find that, although it is possible to match the Lyα/C IV ratio with a value from 3 to 5 eV, only a cutoff energy between 8 and 10 eV can produce the observed change in Si IV/C IV. If the cutoff energy is lower than 8 eV, the high-energy tail of the bump would not extend beyond 30 eV, and both Si IV and C IV would respond to the power-law component. On the other hand, if it is higher than 10 eV, both lines would be dominated by the bump. In either case, the Si IV/C IV ratio should not exhibit a significant change. The small variation scale of N V requires a cutoff energy not more than 8 eV as this line is particularly sensitive to the strength of the soft X-rays. Thus, our estimated parameter E_{eV} is slightly lower than the previous values, allowing a better fit to several other lines. This form of a UV bump apparently does not fit the low-energy end and hence implies a bump shape more complicated than a blackbody curve. We speculate that the UV bump takes a functional form with a more progressive cutoff and possibly consists of multicomponents.

3.2. Mg II *and* Fe II

The Mg II line is characterized by the smallest variation amplitude and lowest ionizing energy. Photoionization models have previously indicated that the Mg II and Fe II emission should originate from a very deep (optically thick to soft ionizing photons) and semi-ionized zone since the ionization potentials of Mg^0 and Fe^0 are significantly less than that of hydrogen and, therefore, their first stage of ionization can be sustained much beyond the ionized zone in which the emission lines from the other ions are excited. For the emissivity of Mg II to be important relatively to other lines, however, a sufficiently high electronic density and temperature are still required. The Mg II emission is therefore very dependent on the physical conditions encountered throughout the semi-ionized zone. This zone is known to be excited and heated mainly by the unabsorbed soft X-rays. Krolik & Kallman (1988) have shown how the Mg II and Fe II emission is associated with soft X-ray photons above 500 eV and, therefore, according to the trends of Table 2, it makes sense that the Mg II line be characterized by the lowest variation amplitude since the photons (indirectly) responsible for its emission are of very high energies.

Moreover, the subtraction of high- and low-state Mg II flux in F9 yields a profile considerably different from that of C IV and Lyα (Zheng & O'Brien 1989). Lub & de Ruiter (1992) find that a very long delay (2 yr) for the optical Fe II emission. These results suggest that the Mg II and Fe II emission may be formed within a geometrically distinct region and is illuminated by a diffuse high-energy continuum. The primary component of the ionizing continuum, mainly the UV bump, therefore is not expected to extend sufficiently to the soft X-ray region to cause the Mg II emission. We conclude that the geometrical structure appropriate for the optically thick region where Mg II and Fe II are formed is more complex than the simple one-zone model adopted here which predicts too little variation (see Fig. 2*b*) compared to the observations (Fig. 2*a*).

It is worth noting that the assumption of a power-law continuum covering from the X-ray to optical band is still an oversimplification. The X-ray and optical flux do not appear to vary exactly in phase (Wamsteker et al. 1985). The delay of $\sim$400 days of infrared flux (Clavel, et al. 1989) with respect to the UV flux also implies complications.

3.4. *Stastical Considerations*

In Figure 3, we plot the EW of emission lines versus continuum flux, for the seven averaged flux levels. The weaker anticorrelation between the EW of Lyα, C III] and Si IV and the continuum level at 1550 Å is expected since these lines essentially respond to the varying UV bump. The C IV line, on the other hand, follows more closely the power-low continuum and hence varies relatively little. As a result, the C IV EW significantly decreases with increasing UV flux.

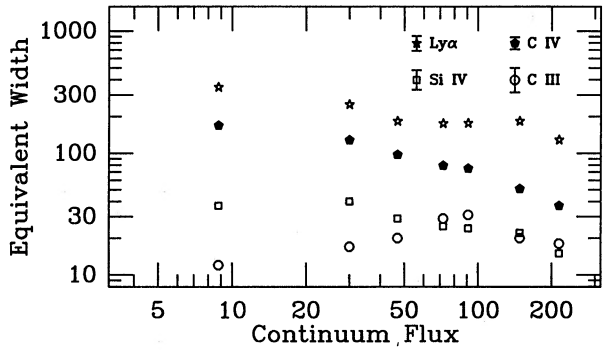

FIG. 3.—Equivalent width (Å) vs. continuum flux at 1338 Å (in 10^{-15} ergs cm^{-2} s^{-1} $Å^{-1}$) in Fairall 9,

To further test this interpretation, we have looked at the possible existence of a similar relation from the statistics of AGNs. We use a sample composed of three subgroups taken from previous studies of the Baldwin effect: Baldwin et al. (1989) for high-redshift quasars, Kinney et al. (1987) for intermediate-redshift quasars, and Wu, Boggess, & Gull (1983) for Seyfert 1 galaxies. Additional Si IV measurements are made from the same *IUE* spectra used in the above publications. Totally 91 objects, including 67 QSOs and 24 Seyfert 1 galaxies have available line fluxes. The whole data set does not constitute a complete sample but nevertheless allows some evaluation of the behavior of the lines.

The luminosity (in magnitude) dependence of EW (in logarithmic scale) are plotted in Figure 4. From Figure 4*a* to 4*d* the plots are in the order of increasing ionization potential. The luminosity-dependence of C IV EW is commonly referred as the Baldwin effect, with a correlation coefficient $r = 0.73$ (logarithmic EW). The correlation coefficient for the Si IV, C III], and Lyα emission is 0.64, 0.52, and 0,40, respectively, indicating a weaker correlation. Given $\log (EW) = A \times M + B$, the slope of regression for C IV, Si IV, C III], and Lyα is 0.091, 0.057, 0.046, and 0.034, respectively. The luminosity-dependence becomes stronger in the order of increasing ionization energy.

Thus the behavior of EW in F9 is similar to that found in the AGN population. We can therefore infer that the C IV/Lyα and C IV/C III] ratios should be characterized by a weak, inverse luminosity-dependence. Such a relation has in fact been noticed by Kinney et al. (1987) and Baldwin et al. (1989). Therefore, both Lyα and C III] become stronger with respect to C IV when the continuum luminosity increases. Also, the contrast between the UV bump and the optical or the soft X-rays should increase with activity level which would lead to a hardening of the UV spectral index at onset of the bump, longward of 1900 Å.

4. SUMMARY

1. In F9, we find a significant change in the UV bump flux between 1826 and 3075 Å. Since the UV bump exhibits a more pronounced variation than the X-ray and optical continuum, the UV continuum is harder at high states. We suggest that the optical and the X-ray flux could be approximated by a single power law originating from a common physical mechanism.

2. Both strong and weak emission lines show differential line variations as the continuum varies. The amplitude of the variations is inversely correlated with the energy of the

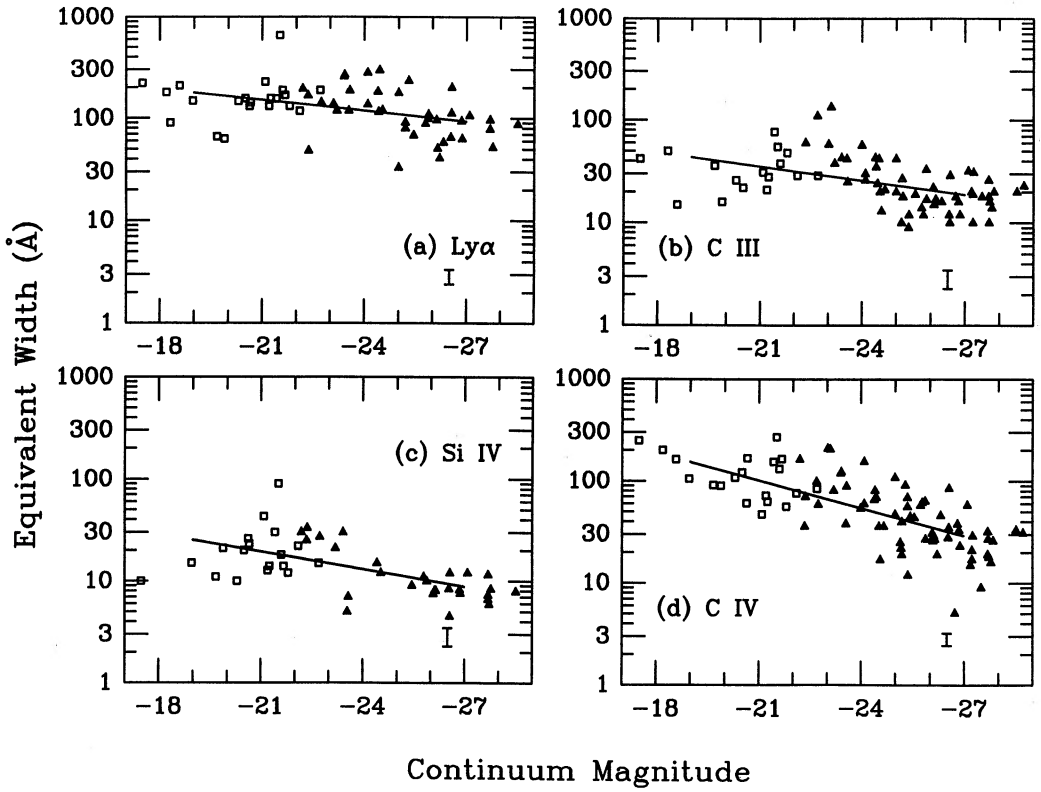

FIG. 4.—Equivalent width vs. continuum magnitude, measured at 1550 Å in the rest-wavelength frame, for 91 Seyfert galaxies and QSOs. *Open square*: Seyfert 1 galaxies; *solid triangle*: quasars. Representative error bars are marked. Note the change in slope of regression line.

photons responsible for exciting the emitting ions. The UV bump appears to affect more directly lines with an ionization potential between 1 and 3 Ry.

3. In the order of increasing ionization potential, the luminosity-dependence of emission-line EW increases. This trend is present not only in F9, but also in the statistics of AGNs. The Baldwin effect is most significant for C IV because the ionizing UV bump generally does not extend beyond 40 eV. An increase level of nuclear activity should be accompanied by a hardening of the UV spectral index.

Since the EUV radiation is still beyond direct access except for a few high-redshift QSOs, more quantitative results may need to wait direct observations from space.

Staff of NASA NSSDC and *IUE* Observatory provided the archival data as well as technical assistance which made our analyses possible. P. T. O'Brien, J. Clavel, C. Ingram, and the anonymous referee are gratefully thanked for their very instructive comments.

This work has been supported by the EPSCoR grant to the University of Alabama, by the Institute for Advanced Study, and by the Research Council of Canada.

REFERENCES

Baldwin, J. A. 1977, ApJ, 214, 679
Baldwin, J. A., Wampler, E. J., & Gaskell, C. M. 1989, ApJ, 338, 630
Binette, L., Prieto, A., Szuszkiewicz, E., & Zheng, W. 1989, ApJ, 343, 135
Binette, L., Robinson, A., & Courvoisier, T.-L. 1988, A&A, 194, 65
Clavel, J., Gilmozzi, R., & Prieto, A. 1988, A&A, 191, 392
Clavel, J., & Santos-Lleó, M. 1990, A&A, 230, 3
Clavel, J., Wamsteker, W., & Glass, I. S. 1989, ApJ, 337, 236
Clavel, J., et al. 1991, ApJ, 366, 64
Kinney, A. L., Huggins, P. J., Glassgold, A. E., & Bregman, J. N. 1987, ApJ, 314, 145
Krolik, J. H., & Kallman, T. R. 1988, ApJ, 324, 714
Lub, J., & de Ruiter, H. R. 1992, A&A, in press
Morini, M., et al. 1986, ApJ, 307, 486
Peterson, B. M., et al. 1991, ApJ, 368, 119
Rees, M. J., Netzer, H., & Ferland, G. J. 1989, ApJ, 347, 640
Wamsteker, W., Alloin, D., Pelat, D., & Gilmozzi, R. 1985, ApJ, 295, L33
Wu, C.-C., Bogess, A., & Gull, T. 1983, ApJ, 266, 28
Zheng, W., & O'Brien, P. T. 1990, ApJ, 356, 463